Geo-Mar Lett
DOI 10.1007/s00367-011-0227-1

ORIGINAL

Small-scale sediment transport patterns and bedform morphodynamics: new insights from high-resolution multibeam bathymetry

Patrick L. Barnard · Li H. Erikson · Rikk G. Kvitek

Received: 8 July 2010 / Accepted: 18 January 2011

Abstract New multibeam echosounder and processing technologies yield sub-meter-scale bathymetric resolution, revealing striking details of bedform morphology that are shaped by complex boundary-layer flow dynamics at a range of spatial and temporal scales. An inertially aided post processed kinematic (IAPPK) technique generates a smoothed best estimate trajectory (SBET) solution to tie the vessel motion-related effects of each sounding directly to the ellipsoid, significantly reducing artifacts commonly found in multibeam data, increasing point density, and sharpening seafloor features. The new technique was applied to a large bedform field in 20–30 m water depths in central San Francisco Bay, California (USA), revealing bedforms that suggest boundary-layer flow deflection by the crests where 12-m-wavelength, 0.2-m-amplitude bedforms are superimposed on 60-m-wavelength, 1-m-amplitude bedforms, with crests that often were strongly oblique (approaching 90°) to the larger features on the lee side, and near-parallel on the stoss side. During one survey in April 2008, superimposed bedform crests were continuous between the crests of the larger features, indicating that flow detachment in the lee of the larger bedforms is not always a dominant process. Assessment of bedform crest peakedness, asymmetry, and small-scale bedform evolution between surveys indicates the impact of different flow regimes on the entire bedform field. This paper presents unique fine-scale imagery of compound and superimposed bedforms, which is used to (1) assess the physical forcing and evolution of a bedform field in San Francisco Bay, and (2) in conjunction with numerical modeling, gain a better fundamental understanding of boundary-layer flow dynamics that result in the observed superimposed bedform orientation.

P. L. Barnard (✉) · L. H. Erikson
Pacific Coastal and Marine Science Center,
United States Geological Survey,
400 Natural Bridges Drive,
Santa Cruz, CA 95060, USA
e-mail: pbarnard@usgs.gov

R. G. Kvitek
Seafloor Mapping Lab, Institute for Earth Systems Science & Policy, California State University,
Monterey Bay, 100 Campus Center,
Seaside, CA 93955-8001, USA

Introduction

The shape, size, migration, and orientation of bedforms can reveal important information about local and regional two-dimensional flow structure, sediment transport processes, and forcing/boundary conditions, including the lateral distribution of net bedload transport direction and the associated residual flow velocity distribution (e.g., Langhorne 1982; Belderson et al. 1982; Kubo et al. 2004). For example, Knaapen et al. (2005) showed that net sediment transport rates as derived from sand wave migration are well correlated with model predictions of residual sediment transport. Some excellent reviews of bedform features and distribution have been published (e.g., Ashley 1990; Dalrymple and Rhodes 1995). For superimposed bedforms, spatial variations in bedform morphology are thought to be due to local flow separation associated with larger bedform morphology, unsteady flows, or possibly secondary flows (cf. Allen and Collinson 1974; Allen 1978). Understanding bedform morphology and controlling processes can provide insight into (1) the fundamental understanding of bedform dynamics in complex hydrodynamic and morphological settings, (2) the influence of boundary condition variations (e.g., sediment supply, sea level rise, tidal forcing) on bedform evolution, and (3)

Published online: 12 February 2011

anthropogenic impacts on bed evolution and sediment transport, which are critical to addressing estuarine sediment management issues such as channel dredging, aggregate mining, and damming.

Allen and Friend (1976) observed bimodal (i.e., superimposed) bedforms over three consecutive sets of spring–neap cycles along the British North Sea coast. In their investigation, over 85% of the superimposed features formed within one-quarter to one-third of a wavelength upstream from the crest of the major bedform. They found the superimposed features to be more three-dimensional, mostly lunate, and abundant only during the spring tidal cycle. The large bedforms were two-dimensional, and more temporally and spatially consistent in size and shape. Terwindt (1971) observed mega-current ripples superimposed at up to 45° angles to the crests of the larger sand waves, with the superimposed height increasing from trough to crest, and suggested that the obliquity was likely evidence that the direction of tidal currents in the bottom boundary layer varied between trough and crest, a result of topographic steering. Dalrymple and Rhodes (1995) note that divergences of up to 90° have been observed, but that 30–60° are more common. Sweet and Kocurek (1990) demonstrated in their study of eolian dunes that the oblique orientation of superimposed bedforms is due to deflection of the near-bed flow by the three-dimensional shape and oblique orientation of the larger dunes, and that when lee-side slopes are <20° flow separation does not occur, but rather stays attached to the bed and is deflected into an along-crest orientation. Ernstsen et al. (2005) observed superimposed bedforms oriented on the lee sides of larger, saddle-shaped bedforms that were oblique to the tidal current directions and perpendicular to larger bedform crests, and attributed their formation to topographic steering as well. Terwindt (1971) also observed superimposed bedforms on either side of the crest oriented toward the crest, the lee-side features referred to as backflow ripples by Allen (1980) that were formed during high flow conditions. Ernstsen et al. (2006a) observed similar features on the lower lee side of large asymmetric bedforms.

Rubin and McCulloch (1980) showed that superimposed bedform heights increase with bed shear velocity. Parsons et al. (2005) performed the first integrated study of detailed three-dimensional flow fields and bedform morphology in a fluvial setting, showing that lateral flows and secondary circulation can have significant impacts on morphology. In their study, superimposed features were absent in the lee-side scour region, and tended to increase in height and wavelength toward the crests of major bedforms. Topographic forcing of flow by the bedforms resulted in differences in flow direction of >15° between flow over the crest and in lee-side areas. Laboratory measurements by Maddux et al. (2003) suggest that the flow deflection could be even higher. Malikides et al. (1989) deployed near-bed current meters on the crest and trough of large (9 m amplitude) subtidal bedforms, and documented current deflection and acceleration over bedform crests associated with the pattern of small superimposed bedform crests at an acute angle to the larger ones. Wienberg et al. (2004) and Wienberg and Hebbeln (2005) quantified the impact of dredge disposal on a bedform field, where, despite significant morphological changes and complete burial in places, there was not a persistent long-term effect, as bedforms regenerated within a few months and continued migrating.

Within the context presented above, large- and small-scale bedform occurrence, shape, and evolution over a seasonal and decadal timescale were investigated in central San Francisco Bay, using recent advances in multibeam echosounder and processing technology from surveys in 2008, and incorporating comparison with earlier, lower-resolution data extracted from a 1997 survey by Dartnell and Gardner (1999). The fine details of the observations from the recent surveys were only possible due to the advance in technology for mapping the seafloor (cf. Ernstsen et al. 2006b), and the associated improvements in post-processing. This paper aims to describe a new technique for resolving the seabed at an extremely fine scale, and explores a direct application of this fine resolution for gaining a better understanding of bedform morphodynamics.

Physical setting

San Francisco Bay, California (Fig. 1), experiences a modest diurnal tidal range (i.e., difference between mean higher high water and mean lower low water) of 1.78 m (NOAA 2010), but due to the size of the estuary over ~7.5 trillion liters of water is forced through the 1.5-km-wide Golden Gate each day, generating tidal currents that can exceed 2.5 m/s in the inlet throat (Barnard et al. 2007). These powerful currents and an ample supply of coarse sediment result in large bedforms that can be up to 317 m in wavelength in the ebb jet (Barnard et al. 2006), with many other large bedforms locally persistent where currents are focused by erosion-resistant bedrock outcrops. By contrast, shorter superimposed bedforms have to date not been recorded in this area, except along spatially restricted, discrete transects using analog side scan in the 1970s by Rubin and McCulloch (1980). Relatively low-resolution (~4 m) surveys performed in 1997 by Dartnell and Gardner (1999) were unable to detect any such features. Barnard and Kvitek (2010) investigated the regional-scale bathymetric change between the surveys conducted in 1997 and 2008, but did not analyze any fine-scale seabed patterns.

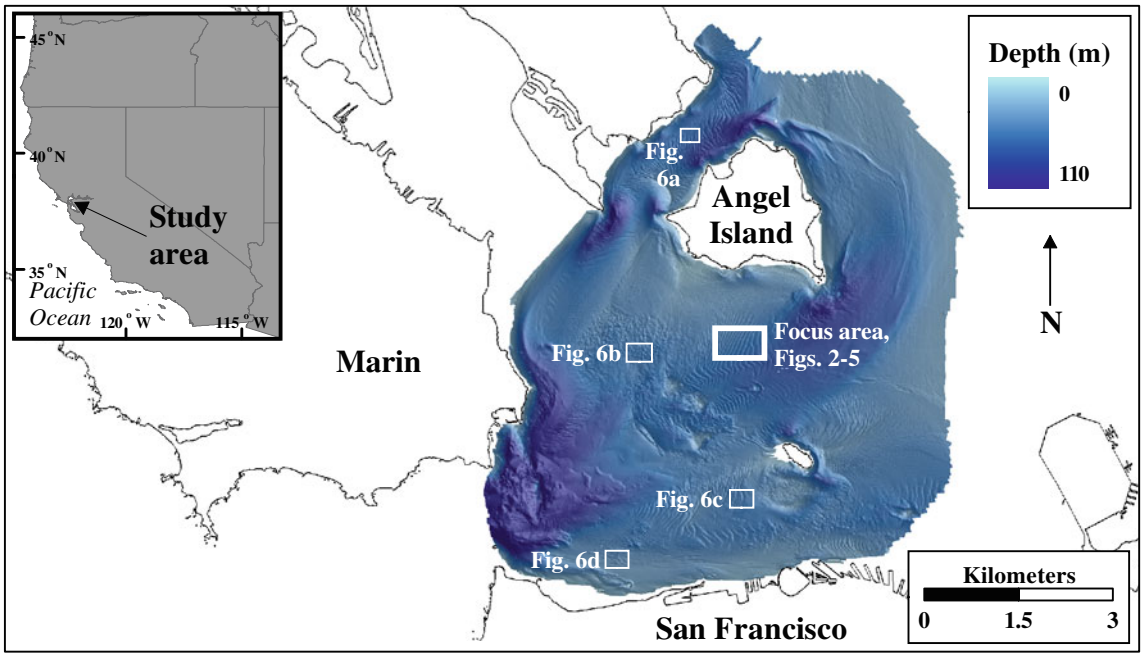

Fig. 1 Location of the study area with depth measurements from the April 2008 survey in shaded relief (sun azimuth=240° and angle=25°). Also shown are the locations of five sites selected for more detailed analyses (*boxes*)

The study was carried out in 2008 in a 1 by 1.5 km bedform field in central San Francisco Bay, south of Angel Island. A 750 by 450 m focus area within this bedform field (Fig. 1), with water depths ranging from ~20 to 30 m, was selected for more detailed analysis of bed characteristics using multibeam bathymetry. This site is located to the east and northeast of highly active aggregate mining sites (Chin et al. 1998), where ~6 million m^3 of sand and gravel was removed from 1997–2008 (Barnard and Kvitek 2010). Median bed grain size in the focus area is 0.35 mm (n=12 grab samples, d_{10}=0.17 mm, d_{90}=1.0 mm; Barnard, unpublished data). Cheng and Gartner (1984) measured currents at 35% and 65% of the local water depth (30 m) at a site about 800 m northeast of the study area. Tidal currents peaked at 1.5 m/s at this site, with an M_2 tidal constituent amplitude of 0.55 m and principal axis orientation of 260° (nautical convention). During the 11 years between surveys, 5 years were wet or above normal, 5 years were dry or below normal, and 2008 was a critical dry year (DWR 2010). Nevertheless, even during high flow years freshwater discharge accounts for less than 1% of the tidal prism, and is not considered to significantly alter boundary-layer hydrodynamics in central San Francisco Bay (Barnard et al. 2007).

Bedforms in the center of the estuary are generally oriented transverse to the dominant tidal current directions, and diverge from the central axis of the flow (Barnard et al. 2010). Local, wind-generated waves and deep ocean swell can induce significant turbulence and sediment transport in the shallower, intertidal sectors of the bay, where fine sediment dominates the substrate (Talke and Stacey 2003). However, they likely play only a minor role in sediment transport in the deeper sectors, including our study area.

Materials and methods

Multibeam bathymetry

Multibeam bathymetry surveys were conducted on 27 April and 19 November 2008. Both were performed during a rising tide and at the tail end of a spring tidal cycle, but the first took place following spring tides with a peak tidal range of only 1.8 m, while the second range was 2.7 m. The study area was mapped using a Reson 8101 multibeam sonar system aboard the R/V *VenTresca* operated by the Seafloor Mapping Lab at California State University, Monterey Bay. The 8101 operates at 240 kHz, and measures relative water depths within a 150° swath consisting of 101 1.5×1.5° beams. It can provide up to 3,000 soundings per second with swath coverage up to 7.4 times the water depth. No data were used beyond 55° from nadir to insure the highest quality and resolution. The surveys were also run at 25% overlap, so the following specs for single track lines are survey coverage minimums:

- Swath coverage: data filtered to 55° from nadir
- Maximum outer beam footprint size at 55°: at 10 m depth=0.8 m, at 20 m=1.6 m, at 30 m=2.4 m
- Minimum ping rate in 30 m water depth was 15/s, which at maximum 10 km/h survey speed=minimum 5

pings per meter along track with swath constrained to 55° from nadir.

The minimum sounding density exceeded the resolution of the gridded data, as demonstrated by the lack of holes in the imagery, because no interpolation was needed due to the very high data density (>>1 sounding per meter).

A CNAV 2050 RTG GPS system supplied real-time position data to an Applanix Position and Orientation System, Marine Vessel (POS/MV 320v4). Horizontal positional accuracy of this system is typically ±15 cm. Attitude (pitch, roll, yaw, and heave) data were generated at 200 Hz by the POS/MV with an average pitch, roll, and yaw accuracy of ±0.03°, while heave accuracy was maintained at ±5% or 5 cm. Surface-to-seafloor profiles of the speed of sound through the water were collected periodically during the surveys to correct for any variations in sound velocity due to salinity and temperature changes throughout the water column.

Sonar data were post-processed using CARIS Hydrographic Information Processing System (HIPS) 6.1 software, after combining with the vessel trajectory and sound velocity data. Vessel trajectory data from the Applanix POS/MV were processed using Applanix POSPAC 5 software and a tightly coupled inertially aided post processed kinematic (IAPPK) technique to generate a smoothed best estimate of trajectory (SBET) file at 200 Hz. The SBET solution includes rotational motion about all three axes, as well as heave due to surface waves and tidal variation over the survey period, all tied directly to the NAD83 ellipsoid (cors96). This technique virtually eliminates positional and motion-related artifacts traditionally found in multibeam data that tend to obscure fine, sub-meter geomorphic detail, particularly when data from adjacent track lines are superimposed. Applying the new IAPPK SBET approach to existing multibeam sonar data yields more co-registered data points per unit area with less noise, bringing fine features into much sharper focus than previously was possible.

Final bathymetric point data were gridded to 1 m for bedform analysis. Bedform measurements (height and wavelength) were made along hand-picked, representative transects oriented orthogonal to bedform crests. Bedform orientation was determined along the crest of each bedform, and asymmetry was calculated as the percentage offset from symmetry based on flank lengths (see Barnard et al. 2010 for additional details on bedform analysis methods).

Numerical modeling

A Deltares Delft3D numerical model (Roelvink and van Banning 1994) was used to investigate hydrodynamic and sediment transport forcing mechanisms that might be responsible for the observed bedforms. The model developed for this study used a 10-layer sigma grid with near-bed layers equaling 6% of the total water depth and encompassing all of San Francisco Bay, the Golden Gate, and the continental shelf to 90 m depth, from Pt. Reyes in the north to more than 60 km south (Barnard et al. 2007). Extensive calibration and validation showed that a large model domain was needed to accurately reproduce high-velocity flows through the Golden Gate, and complex flow patterns in the vicinity of the inlet and within the bay. Four sub-domains (sea, central bay, south bay, and north bay) were employed to allow for local refinement of the central bay sub-domain and the focus area, and to reduce computation time through parallel processing on a quad-core personal computer. Curvilinear grid cell sizes vary from 2 km in the sea domain, to 100 by 10 m (the order of major bedform wavelengths) in the focus area. The open sea boundary was forced with astronomic constituents derived from several calibration iterations of measured and predicted water levels at the San Francisco tide gauge, and current measurements throughout the bay. Boundaries in the delta region of the north bay grid were defined by San Joaquin and Sacramento River freshwater inputs with daily volumetric inflows estimated from the Dayflow model (http://iep.water.ca.gov/dayflow/). For the April 2008 simulation, the model was initiated with a spatially and vertically varying salinity field based on measurements made on 10 January 2008 (USGS, http://sfbay.wr.usgs.gov/cgi-bin/sfbay).

To assess model performance, model-predicted water levels were compared to measurements at the San Francisco tide gauge, resulting in a root-mean-square error of 5 cm. In lieu of actual current measurements in the focus area, tidal constituent amplitudes were calculated via harmonic analysis (Pawlowicz et al. 2002) of currents simulated within the focus area over a 1-month time period (depth-averaged calculations), and compared to those derived by Cheng and Gartner (1984). An average of harmonically derived current amplitudes at all grid cells within the study area indicates an average M_2 amplitude of 0.52 m and a principal axis of 252°. These values compare well with Cheng and Gartner's (1984) amplitude of 0.55 m and principal axis of 260°. Based on the model-predicted current amplitudes, the amplitude of the M_2/M_4 tidal asymmetry is 1:50 and the M_2–M_4 phase difference is 106°. This rather large asymmetry and phase difference implies significant inequality in the flood- and ebb-directed tides.

Results and discussion

Bedform details

Bimodal, multi-scale bedforms are clearly observed in multibeam bathymetry surveys in 2008 (Fig. 2a). In April

2008, large bedforms (~60 m wavelength, 1.5 m amplitude) in the center of the focus area were migrating toward 291° (nautical) along transect A–B (Fig. 2b), while superimposed features (~12 m wavelength, 0.25 m amplitude) were migrating 32° along transect C–D (Fig. 2c), based on the observed asymmetry. Large bedform wavelengths increase to the south and east, likely due to depth effects (deeper to the south and east) and/or spatial gradients in sediment transport. From east to west, superimposed bedforms shift from being oriented near-parallel, to nearly orthogonal to larger bedform crests. Locally, in the lee (i.e., slip face/steep face) of major bedform crests, the superimposed bedforms are nearly orthogonal to the larger features, while on the upper stoss side they most often approach parallel. Moreover, the superimposed bedform crests in the April 2008 survey are continuous from lee to stoss. This suggests that the superimposed features may be controlled regionally by larger-scale circulation patterns, where the difference in orientation with the larger features is a reflection of tidal-phase current vector differences (i.e., ebb vs. flood, neap vs. spring), while locally the orientation of superimposed bedforms is controlled by boundary-layer flow deflection in the lee of the large bedform crests. It is noteworthy that in contrast to the discontinuous superimposed bedforms described in the tidal environment of Allen and Friend (1976) and the fluvial environment of Parsons et al. (2005), instead of flow separation there was flow rotation from transverse at the crest, to nearly parallel in the immediate lee of the crest.

Model results support the hypothesis that superimposed bedforms are controlled by both larger-scale circulation patterns and flow deflection driven by topographic steering. Figure 3 shows near-bed (within 6% of total water depth) current vectors at a time preceding the bedform measurement period in April 2008, and for which current magnitudes resulted in shear stress values in excess of the critical shear stress. The shear stress criterion for initiation

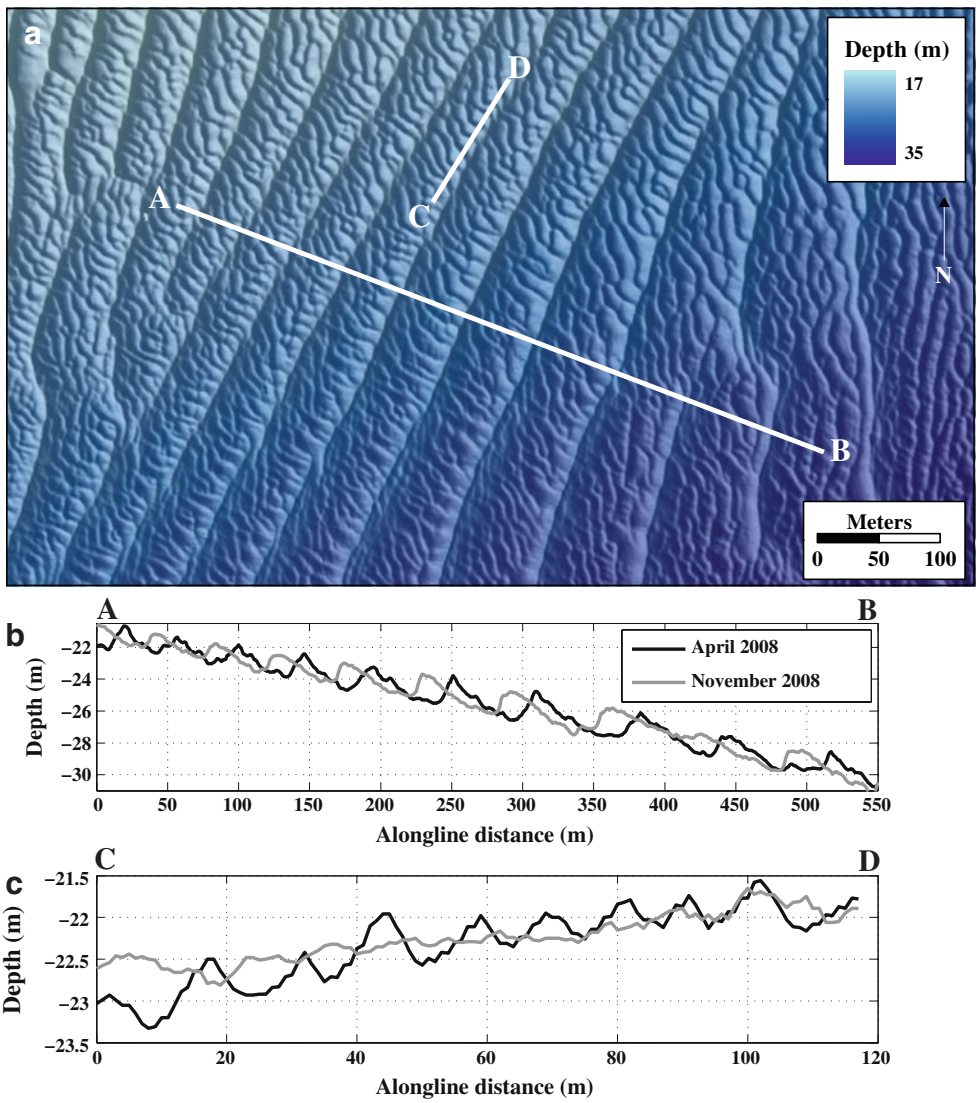

Fig. 2 **a** Bedform focus area colored by depth in shaded relief (sun azimuth=240° and angle=25°) from the April 2008 survey, showing larger as well as superimposed bedforms. **b**, **c** Depth profiles along transect A–B, and along transect C–D from the April and November 2008 surveys. Note the different scales. The regional transport gradients can be viewed in Fig. 5b

of motion and indicative value of relative transport potential, τ_c, was estimated to be 0.29 N/m^2 with

$$\tau_c = \theta_c \rho (s-1) g d$$

where θ_c is the critical Shield's parameter assumed to be 0.05 (e.g., Nielsen 1992), ρ the water density (1,025 kg/m^3), s the relative sediment density (2.65), g the gravitational acceleration (9.81 m/s^2), and d the median sediment grain size diameter (0.35 mm). The ebb event in Fig. 3 suggests sediment mobility to the east and south in the deeper part of the study area, and a relatively greater shear stress at the bedform crests. Velocity vectors and streamlines (not shown) are predominantly transverse to the bedform crests, indicating migration of the large-scale bedforms. Close inspection of the velocity vectors reveal flow deflection at the lee side of the larger dune crests.

Model simulations indicate that streamlines align nearly parallel with the larger bedforms with changing tidal phase (Fig. 4). The near-parallel alignment is due to the larger-scale circulation pattern driven by the tide, regional depth changes, and velocity deflection related to local bathymetric variations. Streamline directions and lower flow velocities indicate the possibility of superimposed bedform generation. Computed bed shear stress values were all less than τ_c during times of streamline alignment with the larger bedforms, however, suggesting either that sediments already in suspension were transported in the along-sand wave direction, or that there were variations in sediment grain size of the surficial versus deeper sediments.

Temporal changes 1997–2008

Decadal change in large-scale features was explored by comparing the 2008 surveys to the 4-m-resolution 1997 survey of Dartnell and Gardner (1999; Fig. 5a–f). Comparison of bedform crests (Fig. 5d) and cross-sections between the 1997 and April 2008 surveys reveals a ~13° shift in bedform crest orientation, a ~40% increase in ebb asymmetry, a 38% increase in bedform height, and an 8% decrease in wavelength in the period 1997–2008. Because flow in the area is unlikely to have changed during this period, these changes are likely explained by large-scale alterations in sediment transport gradients and/or supply. A reduction in sediment supply from the heavy aggregate mining to the southeast (see Physical setting) would explain the shift to ebb transport domination in this region, as well as more rapid bedform migration and thus shifting of bedform orientations along the southern part of the bedform field. Over this time period, the western half of the focus area lost approximately 175,000 m^3 of sediment relative to the eastern half (Fig. 5e).

Temporal changes April–November 2008

Remarkably little change in large bedform morphology occurred between April and November 2008. By contrast, these bedforms actually migrated ~19 m to the west during the 7-month interval, and bedforms in the east of the focus area migrated up to 29% farther than bedforms in the west (Fig. 5f). This suggests an east-to-west flow

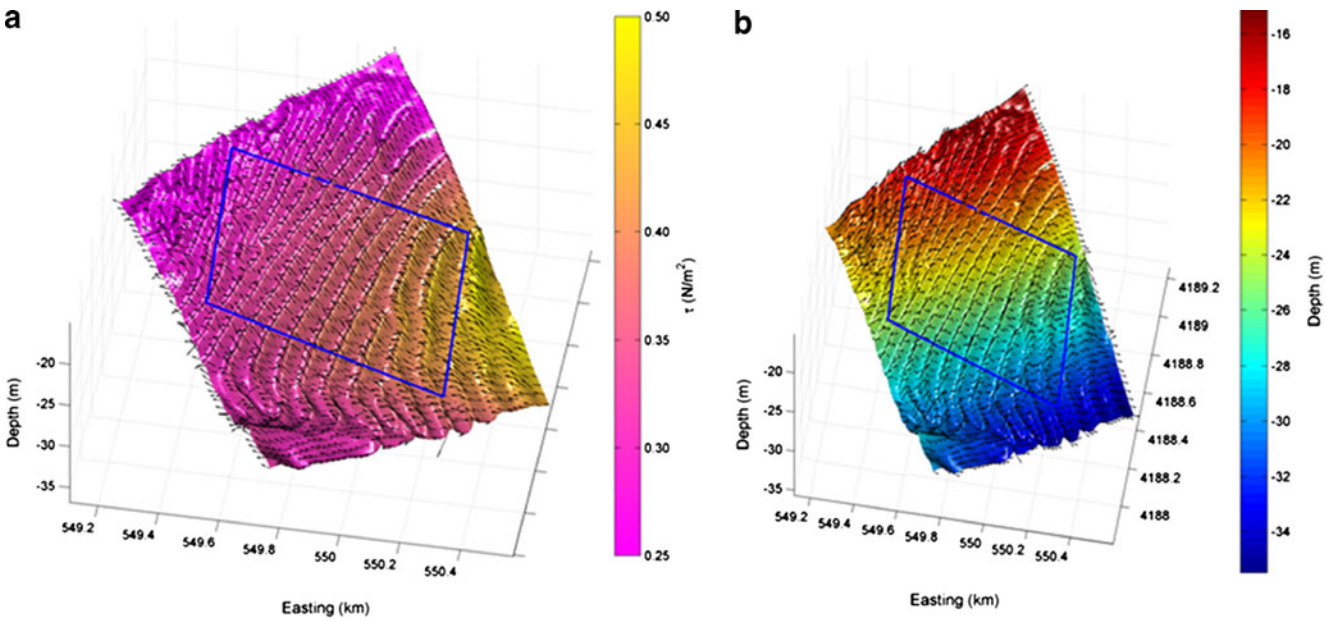

Fig. 3 Velocity vectors calculated with the numerical model during an ebb event on 27 April 2008. Vectors superimposed on **a** bathymetry (elevation) and bed shear stress values (color coded), and **b** color-coded bathymetry. *Blue box* Study area

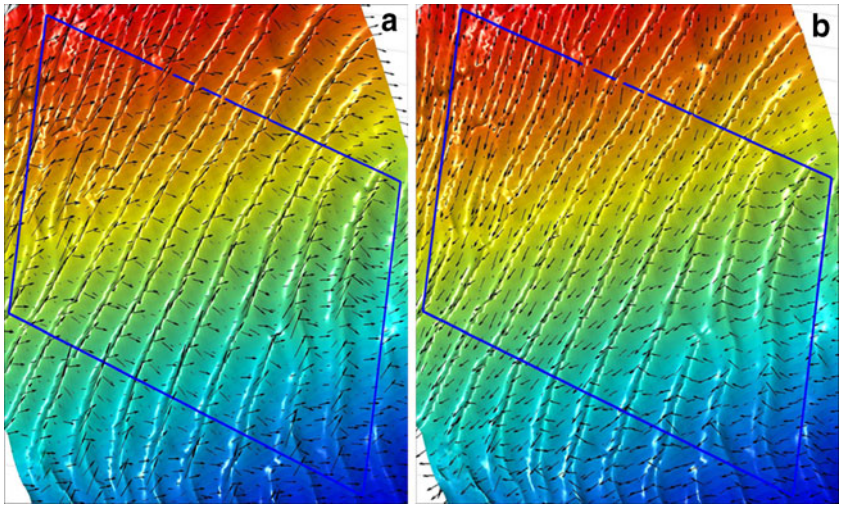

Fig. 4 Velocity vectors calculated with the numerical model during phase change of the tide: **a** approaching flood tide on 27 April 2008 at 08:00 UTC, and **b** approaching ebb tide on 27 April 2008 at 03:40 UTC. Velocity vectors align near-parallel with the larger bedforms as a result of changing tidal phase, regional bathymetry, and topographic steering, and suggest a flow mechanism for the generation of superimposed bedforms. *Blue box* Study area

deceleration that also is consistent with smaller wavelengths, heights, and overall shallowing in the west (Fig. 2). Crests of the large bedforms in April 2008 also are much sharper (i.e., more peaked), better defined, and less asymmetric than in November 2008 (Fig. 2b, c). Alternatively, due to continuity, flow velocity increases to the WNW under steady discharge and a shallowing seafloor. Applying the Bernouilli equation (cf. Terwindt 1971) would lead to an increase in near-bed flow deflection (i.e., refraction) toward the WNW, which is in broad agreement with the change from~crest-parallel to~crest-perpendicular superimposed bedforms relative to the larger bedforms. Therefore, the net bedload transport is predominantly along crest in the WNW, which could also explain the decrease in bedform migration rate and size (V. Ernstsen, personal communication).

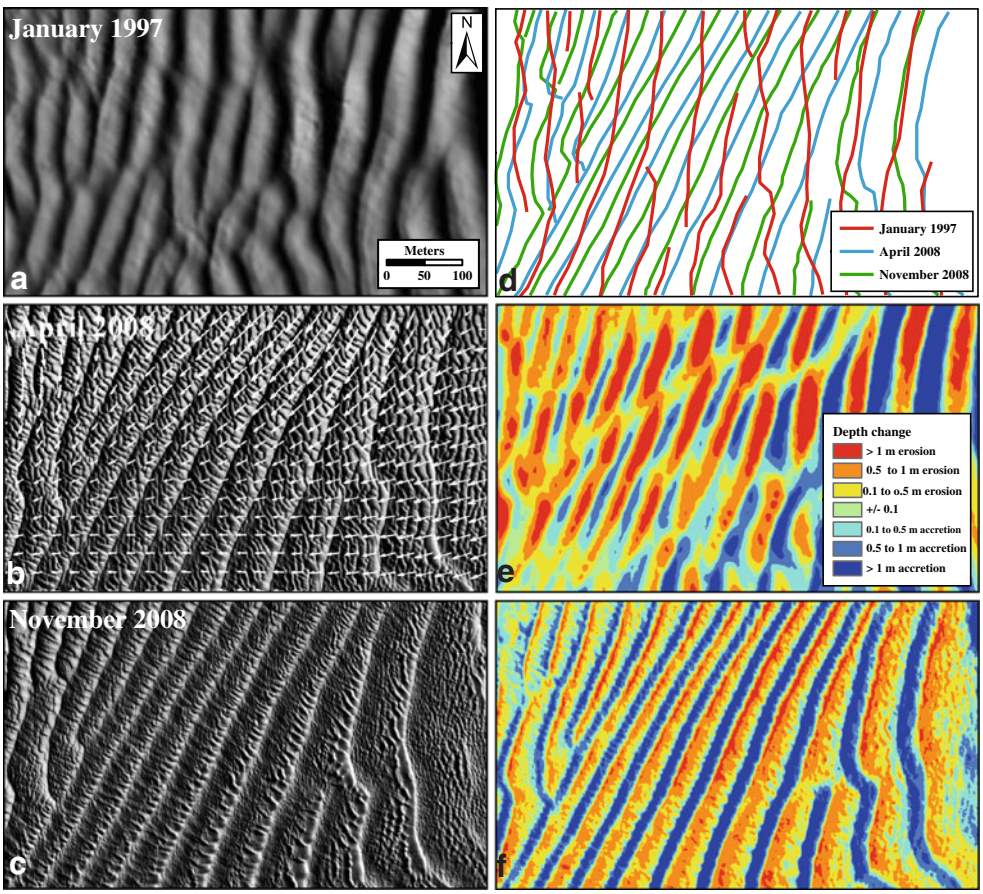

Fig. 5 Multibeam bathymetry in shaded relief (sun azimuth=240° and angle=25°) from the focus area for the **a** January 1997, **b** April 2008, and **c** November 2008 surveys. Panel b includes the model-predicted near-bed sediment transport gradients at maximum predicted ebb tide prior to the April 2008 survey (extracted from Barnard et al. 2010). **d** Crest locations from the three surveys. **e** Depth change from January 1997 to April 2008. **f** Depth change from April to November 2008. The 1997 datasets were extracted from Dartnell and Gardner (1999)

While large-scale features were remarkably well preserved from April to November 2008, superimposed bedforms were significantly different (Fig. 5b, c). Superimposed bedforms were much better developed in April 2008, with continuous crests between adjacent large bedform crests, even on the lee side and in the troughs of the larger features. In the November survey, superimposed bedform crests are discontinuous in the lee of major bedforms, suggesting flow detachment in the lee of the crest. This observation is counter to the observations of Dalrymple and Rhodes (1995); sharper crest peaks in April 2008 did not result in boundary-layer flow detachment, but rather flow deflection into an along-crest orientation, as documented by the commonly transverse-oriented (to the compound bedform crests), superimposed bedform crests that are virtually continuous moving over the crest from the stoss to lee sides (Figs. 2a, 5b). In November 2008, by contrast, with less pronounced compound bedform crests and highly discontinuous superimposed bedforms in the lee of the crests, flow detachment is a dominant process. Allen and Friend (1976) reported a much higher occurrence of superimposed bedforms following larger spring tidal ranges. One explanation may be that bedforms tend to be more three-dimensional at higher flow magnitudes, but only within their stability range. In the Allen and Friend (1976) case, this increase in three-dimensionality occurred during spring tides, but in San Francisco Bay velocities associated with spring tides may exceed stability limits for observed bedforms.

The abundance of well-developed large-scale and superimposed features following the moderate spring tidal cycle of April 2008 thus could be explained by optimal flow conditions for those features, whereas the degraded bedforms observed in November 2008 may reflect flows exceeding the stability regime (i.e., upper plane beds). Threshold velocity for cavitation of the superimposed bedforms was estimated with the numerical model. Ebbing currents up to 55 cm/s are predicted to have occurred prior to the April 2008 survey, indicating that the superimposed bedforms are not cavitated with such velocities. The last peak velocity in excess of 55 cm/s prior to the November 2008 multibeam survey occurred on a flood tide with the preceding ebb tide predicted to have reached 80 cm/s. Maximum currents are predicted to have reached 90 cm/s between the April and November survey, thus suggesting that the threshold velocity for secondary bedform deflation is between 55 and 90 cm/s.

Future applications

New higher-resolution bathymetry has the potential to facilitate investigation of a variety of bed features and contributing processes. In San Francisco Bay, bidirectional flow patterns (Fig. 6a), significant bottom disturbance due to aggregate mining activities (Fig. 6b), transitions to different flow regimes (Fig. 6c), and large-scale flute marks due to dredge mound evolution under largely unidirectional transport (Fig. 6d) can now be viewed in unprecedented detail. This new technology has clear application to understanding anthropogenic influences on the seabed and on sediment transport, and for specific problems such as mine burial studies (e.g., Trembanis et al. 2007).

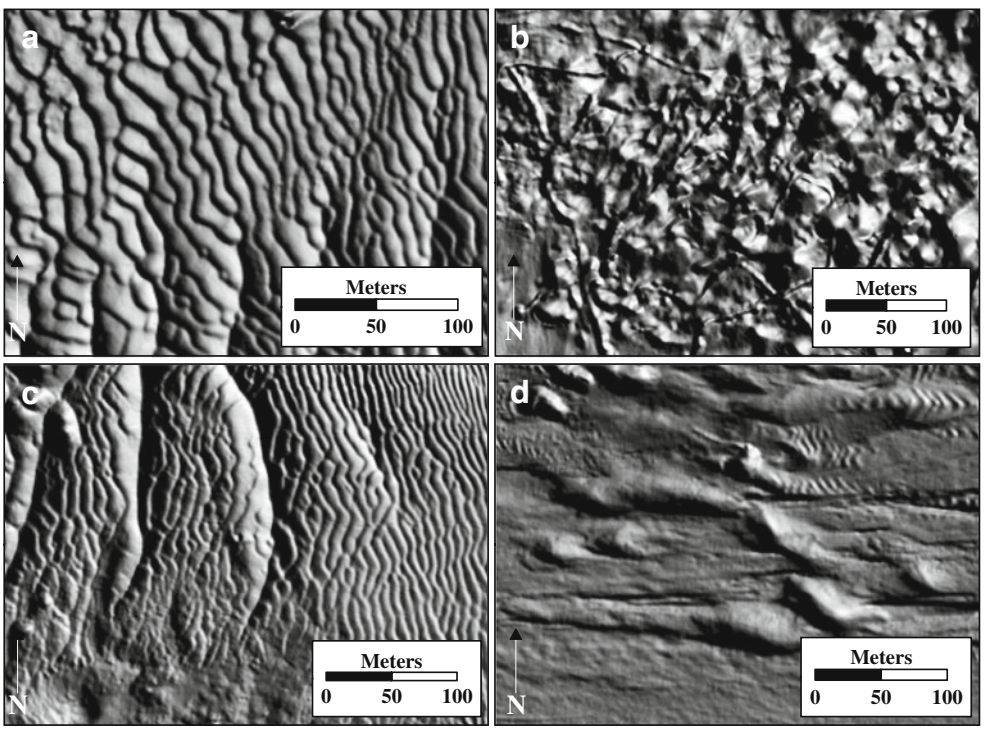

Fig. 6 High-resolution multibeam bathymetry images in shaded relief (sun azimuth=240° and angle=25°) from four selected sites investigated in April 2008 throughout the study area. The location of the panels is shown in Fig. 1. **a** Bidirectional flow patterns, **b** mining disturbances, **c** transition to different flow regimes, and **d** flute marks due to dredge mound evolution

The combination of dramatically improved resolution in multibeam bathymetry combined with hydrodynamic modeling has the potential to better resolve and improve the understanding of seabed morphological change and sediment transport in a variety of marine environments. The current state of the art in sand wave modeling, summarized in Besio et al. (2008), has been successful in predicting large-scale (>50 m) sand wave occurrence, behavior, and evolution. While some laboratory investigations of smaller-scale (<15 m) features exist (e.g., Lacy et al. 2007), superimposed and/or dual-phase features occurring at smaller scales have been largely ignored in models, primarily due to the imaging resolution being insufficient for three-dimensional field testing of models. Today's new bathymetric data, on their own and in combination with other tools such as numerical modeling, will have a variety of applications, including improving defense-based research that relies on predicting small-scale bed changes, and understanding and mitigating anthropogenic activities that modify habitats and sediment transport patterns.

Conclusions

Recent technological improvements to multibeam echosounder systems and processing have increased the potential for resolving and explaining fine details of seabed morphology and sediment transport in a variety of marine environments. In this study, superimposed bedforms (~12 m wavelength, 0.25 m amplitude) not visible in earlier, coarser-resolution surveys and superimposed on large-scale sand waves (~60 m wavelength, 1.5 m amplitude) are identified. Inspection of the data suggests that the superimposed features may be controlled by both regional circulation patterns as well as boundary-layer flow deflection in the lee of the large bedform crests. Comparison between two surveys obtained in April and November 2008 reveals degradation of the superimposed bedforms following spring tides of greater amplitude than in April. In lieu of measurements, numerical model results indicate the threshold velocity to be between 55 and 90 cm/s for secondary bedform deflation (d_{50}=0.35 mm). Model results also support the hypothesis that gradients of sediment transport rates drive large-scale bedform migration patterns, and that superimposed bedforms are the result of tide phase changes, and regional and local variations in the bathymetry resulting in topographic steering. Multibeam bathymetry measurements obtained 11 years apart reveal significant changes in the shape and size of the large-scale sand waves. Because alterations of the gross flow patterns are unlikely, these changes are thought to be related to other factors such as modifications of sediment supply. Boundary-layer flow dynamics are exceedingly complex and change over small spatial scales; increased bathymetric resolution thus is essential to obtaining field data that can be used to test models.

Acknowledgements The authors wish to thank the U.S. Geological Survey and the San Francisco Bay Conservation and Development Commission for funding this research. Gary Greene and Verner Ernstsen provided excellent reviews. In addition, Dr. Ernstsen suggested other plausible explanations for the observed bedform orientations, which were incorporated in the text. Daniel Hoover, Jonathan Warrick and Dave Rubin provided helpful internal reviews.

References

Allen JRL (1978) Polymodal dune assemblages: an interpretation in terms of dune creation-destruction in periodic flows. Sed Geol 20:17–28

Allen JRL (1980) Sand waves: a model of origin and internal structure. Sed Geol 26:281–328

Allen JRL, Collinson JD (1974) The superimposition and classification of dunes formed by unidirectional aqueous flows. Sed Geol 12(3):169–178

Allen JRL, Friend PF (1976) Changes in intertidal dunes during 2 spring-neap cycles, lifeboat station bank, wells-next-sea, Norfolk (England). Sedimentology 23(3):329–346

Ashley GM (1990) Classification of large-scale subaqueous bedforms: a new look at an old problem. J Sed Petrol 60:160–172

Barnard PL, Kvitek RG (2010) Anthropogenic influence on recent bathymetric change in west-central San Francisco Bay. San Francisco Estuary and Watershed Science 8(3), 13 pp, http://escholarship.org/uc/item/6k3524hg

Barnard PL, Hanes DM, Rubin DM, Kvitek RG (2006) Giant sand waves at the mouth of San Francisco Bay. Eos Trans Am Geophys Union 87:285,289. doi:10.1029/2006EO290003

Barnard PL, Eshleman J, Erikson L, Hanes DM (2007) Coastal processes study at Ocean Beach, San Francisco, CA: summary of data collection 2004–2006. U.S. Geological Survey Open-File Rep 2007–1217

Barnard PL, Hanes DM, Erikson LH, Rubin DM, Dartnell P, Kvitek RG (2010) Analyzing bedforms mapped using multibeam sonar to determine regional bedload sediment transport patterns in the San Francisco Bay coastal system. In: Li MZ, Sherwood CR, Hill PR (eds) Sediments, morphology and sedimentary processes on continental shelves. Sedimentology Spec Publ, International Association of Sedimentologists, Blackwell, London, 33 pp (in press)

Belderson RH, Johnson MA, Kenyon NH (1982) Bedforms. In: Stride AH (ed) Offshore tidal sands, processes and deposits. Chapman and Hall, London, pp 27–57

Besio G, Blondeaux P, Brocchini M, Hulscher SJMH, Idier D, Knaapen MAF, Nemeth AA, Roos PC, Vittori G (2008) The morphodynamics of tidal sand waves: a model overview. Coastal Eng 55:657–670. doi:10.1016/j.coastaleng.2007.11.004

Cheng R, Gartner JW (1984) Tides, tidal and residual currents in San Francisco Bay, California—Results of measurements. 1979–1980. Part IV. Results of measurements in central bay region. U.S. Geological Survey, Water Resources Investigations Rep 84-4339

Chin JL, Carlson PR, Wong FL, Cacchione DA (1998) Multibeam data and socio-economic issues in west-central San Francisco Bay (CA). U.S. Geological Survey Open-file Rep 98–139

Dalrymple RW, Rhodes RN (1995) Estuarine dunes and bars. In: Perillo GME (ed) Geomorphology and sedimentology of estuaries. Elsevier, Amsterdam, pp 359–422

Dartnell P, Gardner JV (1999) Sea-floor images and data from multibeam surveys in San Francisco Bay, Southern California, Hawaii, the Gulf of Mexico, and Lake Tahoe, California-Nevada. USGS Digital Data Series, DDS-55, CD-ROM, http://pubs.usgs.gov/dds/dds-55/pacmaps/sf_data.htm

DWR (2010) DAYFLOW calculations. Department of Water Resources, Sacramento, CA, http://cdec.water.ca.gov/cgi-progs/iodir/wsihist

Ernstsen VB, Noormets R, Winter C, Hebbeln D, Bartholomä A, Flemming BW, Bartholdy J (2005) Development of subaqueous barchanoid-shaped dunes due to lateral grain size variability in a tidal inlet channel of the Danish Wadden sea. J Geophys Res 110: F04S08. doi:10.1029/2004JF000180

Ernstsen VB, Noormets R, Hebbeln D, Bartholomä A, Flemming BW (2006a) Precision of high-resolution multibeam echo sounding coupled with high-accuracy positioning in a shallow water coastal environment. Geo-Mar Lett 26(3):141–149. doi:10.1007/s00367-006-0025-3

Ernstsen VB, Noormets R, Winter C, Hebbeln D, Bartholomä A, Flemming BW, Bartholdy J (2006b) Quantification of dune dynamics during a tidal cycle in an inlet channel of the Danish Wadden Sea. Geo-Mar Lett 26(3):151–163. doi:10.1007/s00367-006-0026-2

Knaapen MAF, van Bergen Henegouw CN, Hu YY (2005) Quantifying bedform migration using multi-beam sonar. Geo-Mar Lett 25(5):306–314. doi:10.1007/s00367-005-0005-z

Kubo Y, Soh W, Machiyama H, Tokuyama H (2004) Bedforms produced by the Kuroshio Current passing over the northern Izu Ridge. Geo-Mar Lett 24(1):1–7. doi:10.1007/s00367-003-0134-1

Lacy JR, Rubin DM, Ikeda H, Mokudai K, Hanes DM (2007) Bedforms created by simulated waves and currents in a large flume. J Geophys Res 112:C10018. doi:10.1029/2006JC003942

Langhorne DN (1982) A study of the dynamics of a marine sandwave. Sedimentology 29:571–594

Maddux TB, McLean SR, Smith JD (2003) Turbulent flow over three-dimensional dunes: 1. Free surface and flow response. J Geophys Res 108:6009. doi:10.1029/2003JF000017

Malikides M, Harris PT, Tate PM (1989) Sediment transport and flow over sandwaves in a non-rectilinear tidal environment: Bass Strait, Australia. Cont Shelf Res 9(3):203–221

Nielsen P (1992) Coastal bottom boundary layers and sediment transport. In: Advanced Series on Ocean Engineering, vol 4. World Scientific Publication, Singapore.

NOAA (2010) Tides & Currents. National Oceanic and Atmospheric Administration, Center for Operational Products and Services, http://tidesandcurrents.noaa.gov/

Parsons DR, Best JL, Orfeo O, Hardy RJ, Kostaschuk R, Lane SN (2005) Morphology and flow fields of three-dimensional dunes, Rio Parana, Argentina: results from simultaneous multibeam echo sounding and acoustic Doppler current profiling. J Geophys Res 110:F04S03. doi:10.1029/2004JF000231

Pawlowicz R, Beardsley B, Lentz S (2002) Classical tidal harmonic analysis including error estimates in MATLAB using T_TIDE. Computers Geosci 28:929–937

Roelvink JA, van Banning GKFM (1994) Design and development of Delft3D and application to coastal morphodynamics. In: Verwey A, Minns AW, Babovic V, Maksimovic C (eds) Proc Hydroinformatics'94. Balkema, Rotterdam, pp 451–455

Rubin DM, McCulloch DS (1980) Single and superimposed bedforms: a synthesis of San Francisco Bay and flume observations. Sed Geol 26:207–231

Sweet ML, Kocurek G (1990) An empirical model of aeolian dune lee-face airflow. Sedimentology 37:1023–1038

Talke SA, Stacey MT (2003) The influence of oceanic swell on flows over an estuarine intertidal mudflat in San Francisco Bay. Estuarine Coastal Shelf Sci 58:541–554. doi:10.1016/S0272-7714(03)00132-X

Terwindt JHJ (1971) Sand waves in the Southern Bight of the North Sea. Mar Geol 10:51–67

Trembanis AC, Friedrichs CT, Richardson MD, Traykovski P, Howd PA, Elmore PA, Wever TF (2007) Predicting seabed burial of cylinders by wave-induced scour: application to the sandy inner shelf off Florida and Massachusetts. IEEE J Oceanic Eng 32:167–183

Wienberg C, Hebbeln D (2005) Impact of dumped sediments on subaqueous dunes, outer Weser Estuary, German Bight, southeastern North Sea. Geo-Mar Lett 25(1):43–53. doi:10.1007/s00367-004-0202-1

Wienberg C, Dannenberg J, Hebbeln D (2004) The fate of dumped sediments monitored by a high-resolution multibeam echosounder system, Weser Estuary, German Bight. Geo-Mar Lett 24(1):22–31. doi:10.1007/s00367-003-0155-9